JOURNAL OF SPACECRAFT AND ROCKETS
Vol. 32, No. 3, May–June 1995

Application of Direct Simulation Monte Carlo to Satellite Contamination Studies

Didier F. G. Rault*
NASA Langley Research Center, Hampton, Virginia 23681
and
Michael S. Woronowicz†
ViGYAN, Inc., Hampton, Virginia 23666

A novel method is presented to estimate contaminant levels around spacecraft and satellites of arbitrarily complex geometry. The method uses a three-dimensional direct simulation Monte Carlo algorithm to characterize the contaminant cloud surrounding the space platform, and a computer-assisted design preprocessor to define the space-platform geometry. The method is applied to the Upper Atmosphere Research Satellite to estimate the contaminant flux incident on the optics of the halogen occultation experiment (HALOE) telescope. Results are presented in terms of contaminant cloud structure, molecular velocity distribution at HALOE aperture, and code performance.

Nomenclature

t = surface temperature, °C
ϕ = outgassing flux rate, g/cm^2-s

I. Introduction

ON-ORBIT contamination of satellites and spacecraft due to surface outgassing, equipment venting, and thruster plumes can adversely affect the operation of onboard sensitive equipment such as optical telescopes, radiators, and solar panels. In the design stage of satellite and spacecraft development, an accurate evaluation of contamination levels is necessary, and tradeoff studies are made to properly position instrumentation on the space platform, design appropriate shields, and identify optimum modes of operation of each onboard instrument. The industry standard tools that are used to make such studies are mostly analytical, relying on line-of-sight view factors and ad hoc simulation of intermolecular collisions within the contaminant cloud.[1] As shown in Sec. II, contamination physics and dynamics are very complex and not yet well characterized, and the present simulation methods are known to be very approximate and, at times, inadequate.

An alternative method, which consists in simulating the gas flowfield surrounding the satellite and thence evaluating the contaminant fluxes incident on sensitive surfaces, is presented in this article. The method relies on the direct simulation Monte Carlo (DSMC) algorithm of Bird.[2] This algorithm, which has been extensively used to simulate low-density, high-Knudsen-number flowfields, is described in Sec. III. DSMC has not yet been used in spacecraft contamination studies, mainly because of its high computing costs and the inherently complex geometry of typical satellites. The computing power of present engineering workstations, together with the specific DSMC and CAD methods developed herein and presented in Secs. IV and V, makes it possible now to use DSMC for in-depth contamination studies in reasonably short turnaround times for even the most complex geometry satellites. An example of such a study is described in Sec. VI, where DSMC is used to characterize the contaminant cloud around Upper Atmosphere Research Satellite (UARS) and to evaluate the contaminant flux incident on the aperture of one of its instruments, namely HALOE. Results are compared with the ones obtained with the industry standard contamination code MOLFLUX. The present DSMC-based method yields deposition levels on HALOE optics that are significantly lower than those predicted by MOLFLUX, which corroborates on-orbit measurements revealing little optical degradation in the HALOE field of view.

II. Contamination Physics and Issues

Spacecraft and satellites tend to surround themselves with their own artificial atmosphere as their surfaces emit gases through outgassing, equipment venting, and attitude-thruster firing. This artificial atmosphere is typically of low overall density, which makes it nonisotropic and non-Maxwellian. It is composed of atomic and molecular species with a wide range of molecular weights, including massive long-chain volatile molecules, and a wide range of concentrations, with some critical species being present at trace levels.

The molecular flux of contaminants incident upon a spacecraft surface has traditionally been subdivided into two components: direct flux and return flux. Direct flux from surface A to surface B refers to the molecules flowing from A to B, either along the line of sight or through multiple surface reflections. Return flux to surface A refers to contaminant molecules that are reflected back to A either through self-scattering or through collisions with other molecules in the gas cloud. Computation of the direct flux is fairly straightforward for diffuse Lambertian surfaces (through geometric view factors or particle tracing), but computation of the return flux, which requires an integrated knowledge of the contaminant cloud structure and collision physics, is intrinsically more complex. The latter also requires a relatively large computational domain to be constructed around the spacecraft to insure that the simulation takes account of all the molecules that can return to the vehicle surface, regardless of how far they traveled before being scattered back.

The physics involved in contamination, with regard to surface desorption, reflection, absorption, adsorption, etc., are very complex. The experimental data base is presently insufficient to devise accurate models to simulate mechanisms such as surface outgassing (flux magnitude as a function of surface temperature and material composition, emitted molecule velocity distribution and species composition), surface deposition and polymerization (effect of the sun's ultraviolet radiation, atmospheric monatomic oxygen flux and surface material), and surface reflection (momentum and energy

Presented as Paper 93-0724 at the AIAA 31st Aerospace Sciences Meeting, Reno, NV, Jan. 11–14, 1993; received Feb. 10, 1993; revision received April 20, 1994; accepted for publication July 26, 1994.

*Aero-Space Technologist, Aerothermodynamics Branch, Gas Dynamics Division.
†Research Engineer.

accommodation). Reliable estimates of contamination levels around future spacecraft will therefore require improving the present state of knowledge. The molecule-based DSMC algorithm is readily amenable to incorporation of new physical models as these become available. DSMC could therefore be used to evaluate these models and henceforth foster new research in this field.

III. Direct Simulation Monte Carlo Approach

In engineering studies, DSMC is commonly used as a flow simulation code whenever the flowfield is in the transition regime, i.e., when the characteristic Knudsen number of the flowfield is in the range[3] of 0.01 to 10. Such conditions arise, for example, in the case of re-entry vehicles at high altitudes, such as[4] the Space Shuttle in the altitude range of 170 to 100 km. At these flow conditions, the gas no longer behaves as a Maxwellian continuum fluid, and nonequilibrium may exist in all energy modes, i.e., in vibrational, rotational, and even in translational modes. The gas is typically anisotropic, which means that it can no longer be characterized by a single temperature and the molecular velocity distribution is no longer Maxwellian. To simulate flowfields in this regime, conventional computational fluid dynamics (CFD) numerical tools, which are based on solving the Navier–Stokes equations, cannot be used. Instead, the gas is simulated as a large ensemble of discrete molecules, and computers are used to track a representative sample of these molecules as they move through a computational domain and collide with each other and solid surfaces. The computational domain is subdivided into a grid of cells, the size of which is on the order of the local collision mean free path. The molecular velocity distribution is evaluated within each cell and its moments are evaluated to obtain the species density (zeroth moment), the flow mean velocity (first moment), and the temperature in each of the three spatial directions (second moments).

IV. Three-Dimensional DSMC Code—Features and Applications to Contamination Studies

The three-dimensional DSMC code used in the present study was devised by Bird[5] and further developed by Rault.[4,6–9] High computational and setup efficiencies are achieved through the use of an unstructured grid overlaid on a cubic Cartesian mesh, as shown in Fig. 1, which depicts the computational grid used for the UARS satellite contamination analysis. The code has previously been used to simulate flowfields surrounding slender hypersonic vehicles,[6,7] blunt re-entry vehicles,[8] and spacecraft,[9] and in various other studies such as the flow past a compression corner[10] and freestream-jet interactions.[11] Good agreement has been shown to exist between code predictions and wind-tunnel or flight data, when available. The code has been complemented with a set of utilities for graphical diagnosis, preprocessing, postprocessing, and grid adaptation.

For contamination studies, the code has been implemented on parallel processors. The computational domain is subdivided into two domains, corresponding to the satellite near field ("inner domain") and far field ("outer domain"). The outer domain is necessary to assess the relative importance of the return flux due to intermolecular collisions far away from the satellite. This two-domain methodology allows one to define the satellite surface at as high a spatial resolution as possible while still considering a large enough volume around the satellite to take proper account of the return flux. Two separate simulations, corresponding to the inner and outer domains, are run in a parallel mode on two different processors. The Oak Ridge National Laboratory PVM software[12] is used to transfer information between the two processors at every time step.

To avoid the need for molecule removal or multiplication at the domain interface, the simulation time-step DTM and simulated molecule weight factor FNUM in either domain are set up so that

$$\mathrm{FNUM}_i/\mathrm{DTM}_i = \mathrm{FNUM}_o/\mathrm{DTM}_o$$

where subscripts i and o, respectively, refer to the inner and outer domains.

Due to the large variation in species concentration within a contaminant cloud, weight factors were implemented to artificially

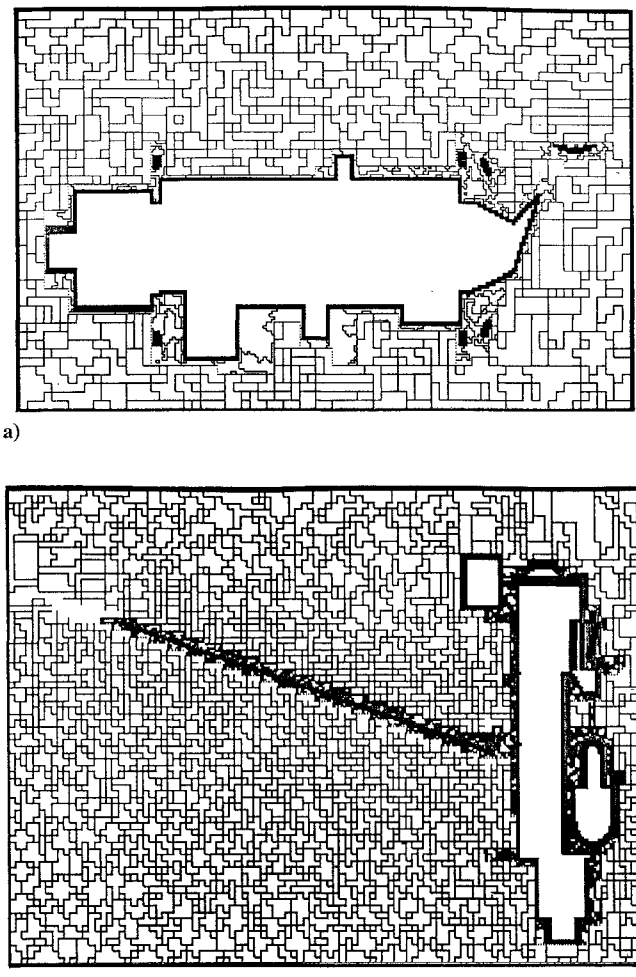

Fig. 1 Computational grid around UARS: inner-domain cross sections at a) $Z = 0$ and b) $Y = 0.5$ m.

enhance minor-species concentrations. The critical species, such as the long-chain molecules, which are most likely to deposit and polymerize on optical surfaces, are usually present in trace amounts, and statistics on these molecules would therefore be inadequate without the use of species weight factors. The DSMC code has been modified by increasing the outgassing flux of trace species by a factor f and decreasing the collision cross section of these species by the same factor f.

V. CAD Geometric Preprocessor

To define and input the inherently complex geometry of typical satellites, the interactive three-dimensional CAD preprocessor developed by Rault[9] is used. This preprocessing utility relies on the fact that even a very complex body geometry can be decomposed into a series of simple geometric primitives, such as spheres, cylinders, planes, etc., or parts thereof. Table 1 shows a list of the 16 basic primitives currently available. The geometric properties of each subcomponent of a spacecraft are entered into the preprocessor through an editable spreadsheet, a sample of which is reproduced in Table 2. The spreadsheet consists of a set of records corresponding to the satellite subcomponents, and each record is composed of a series of fields. These fields describe the nature of the subcomponent, its dimensions and coordinates. The preprocessor creates a graphic file in a format that can be visualized on most engineering desktop workstations and initializes the DSMC code. Figure 2 shows the UARS spacecraft as viewed by the CAD preprocessor.

The outgassing characteristics of each of the satellite subcomponents are entered in a similar way, using a spreadsheet to store information on the subcomponent outgassing flux rates,

Table 1 Library of geometric primitives

Primitive	Definition	Inputs
Sphere A	Complete sphere	Radius, center
Sphere C	Spherical arc	Point, direction, depth
Sphere D	Spherical section	Point, direction, depth, two radii
Sphere E	Hemisphere	Point, direction, radius
Cylinder A	Right cylinder	Two points, radius
Cylinder B	Right cylinder	Two points, radius, direction, length
Cylinder C	Skewed cylinder	Two points, radius, two directions
Cone A	Right cone	Half angle, apex, direction, length
Cone B	Right cone	Apex, direction, length, exit radius
Cone C	Right cone	Point, half angle, direction, length, radius
Cone D	Frustum	Point, direction, length, two radii
Plate A	Triangular plate	Three points, direction
Plate B	Four-sided plate	Four points, direction
Disk	Circular disk	Center, direction, radius
Ring A	Concentric ring	Center, direction, two radii
Ring B	Ring between circle and rectangle	Center, direction, height, width, radius

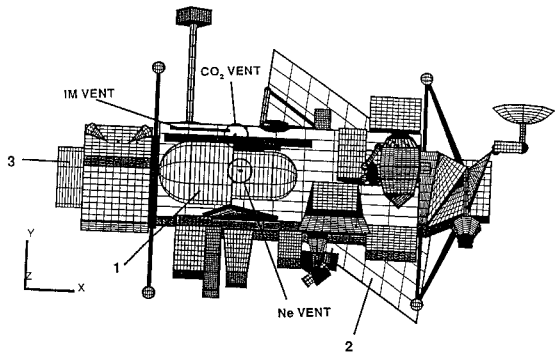

a)

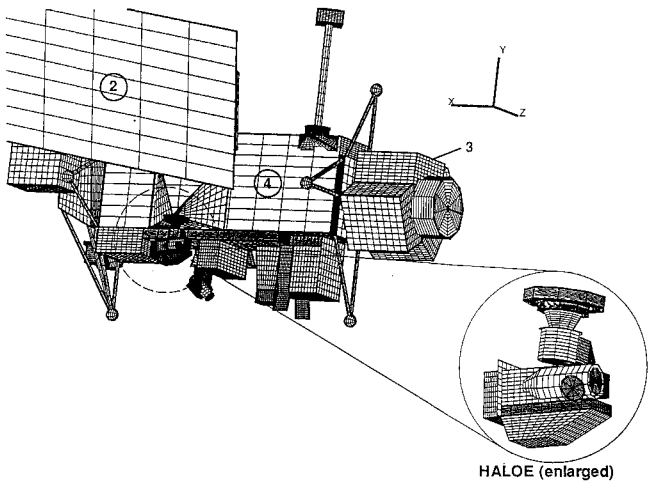

b)

Fig. 2 CAD preprocessor representation of UARS: a) +Z side, case 1 and b) −Z side, case 1. Key: 1, cryogenic limb array etalon spectrometer (CLAES); 2, solar panel; 3, multimission modular spacecraft (MMS); 4, instrument module (IM).

Table 2 Geometry input data spreadsheet

Data			Description
27	347		No. of data planes, quadrics
0.0254			Scale
	Main block top plate (plate B)		
1			Flow is outward
3	48.1	−42.5	Point A
218	48.1	−42.5	Point B
3	48.1	2.1	Point C
218	48.1	−20.0	Point D
100	50.0	−20.0	Exterior point
	CLAES small cylinder (cylinder A)		
1			Flow is outward
64.5	2.7	306.0	Point A
97.1	2.7	30.6	Point A
20.0			Radius

species composition, temperature, and outgassing surface coordinates. These outgassing characteristics can also be visualized graphically in a format similar to the one used for the CAD geometry file.

VI. Application of DSMC to UARS/HALOE Contamination Analysis

UARS/HALOE Description

UARS was designed to collect data on various aspects of Earth's upper atmosphere to help characterize global atmospheric changes that are presently thought to be occurring. It is operating at an altitude of 600 km in a quasicircular orbit. UARS is about 10.3 m long, 5.9 m high, and 3.2 m wide, and its solar panel is 13.3 by 3.3 m. Several instruments have been mounted on the spacecraft bus, including HALOE, the cryogenic limb array etalon spectrometer (CLAES), and the Multimission Modular Spacecraft (MMS). During each sunrise and sunset experienced by the satellite, the HALOE telescope peers at the sun through the atmosphere and measures infrared energy absorption, from which the vertical concentrations of trace halogen gases and ozone are deduced. UARS has an orbital period of 96 min, during which time HALOE is operational and sun-tracking for only 15 min and in a stow position facing free space for the rest of the time. For precise measurements, HALOE optics must remain extremely clean and free of contaminant.

There are four main sources of gas that contribute to the artificial atmosphere enveloping UARS:

1) The ambient atmosphere, which flows past UARS at a relative velocity of 7500 m/s.

2) The CLAES vents, which discharge neon and carbon dioxide at rates of 4.14×10^{-4} and 7.20×10^{-4} g/cm^2-s, respectively.

3) The spacecraft bus instrument vent, Instrument Module (IM), which is located above CLAES and discharges volatile long-chain molecules at an assumed rate of 1.60×10^{-7} g/cm^2-s

4) The thermal protection blankets Multi Layer Insulation (MLI), the painted surfaces, and the solar-cell adhesive, which also outgas long-chain molecules at rates that depend on the surface material composition and temperature.

Computation Conditions and Assumptions

A series of computations has been performed to characterize the contaminant cloud for the spacecraft configurations corresponding to the following conditions:

Case 1: End of HALOE sunrise data collection period.

Case 2: Start of HALOE sunrise data collection period.

Case 3: HALOE in nominal stow position.

The solar panel and HALOE telescope angular orientations for these conditions are listed in Refs. 13 and 14. In each case, the ambient atmosphere was assumed to be composed of 100% monatomic oxygen at a density of 6.0×10^{12} molecules/m^3. Three fictitious species were created to represent the heavy organic molecular contaminant, with molecular weights of 100, 150, 200, as shown in Table 3, which lists the outgassing sources and fluxes for each gas species. The outgassing flux rates were measured during a month-long bakeout test[14] conducted at a reference temperature of 100°C. The temperature

Table 3 Outgassing species[a]

Item	GMW, g	Molecular diam, Å	Mass flux rates at 100°C, g/cm^2-s
Fictitious organic volatile species representing products from MLI	100	5.33	4.33×10^{-13} to 6.01×10^{-12}
Fictitious organic volatile species representing products from solar array adhesives	100	5.33	1.83×10^{-10}
Fictitious organic volatile species representing products from IM and MLI vents	100	5.33	1.60×10^{-7} (IM) 1.22×10^{-8} (MLI)
Fictitious organic volatile species representing products from MMS vents	100	5.33	3.67×10^{-11} to 1.22×10^{-10}
Fictitious organic volatile species representing products from Chemglaze	150	6.33	7.70×10^{-11}
Fictitious organic volatile species representing products from S/13G/LO-VIO	200	6.96	4.30×10^{-11} to 5.39×10^{-11}
Neon vented from CLAES experiment	20.18	2.72	4.14×10^{-4}[b]
Carbon dioxide vented from CLAES experiment	44.01	5.41	7.20×10^{-4}[b]

[a]Reference 14.
[b]Rate at operating temperature $T_{exit} = 207$ K.

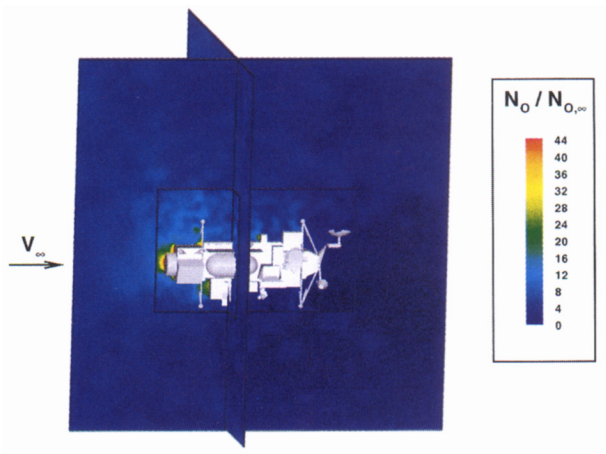

Fig. 3 Atmospheric oxygen density map around UARS.

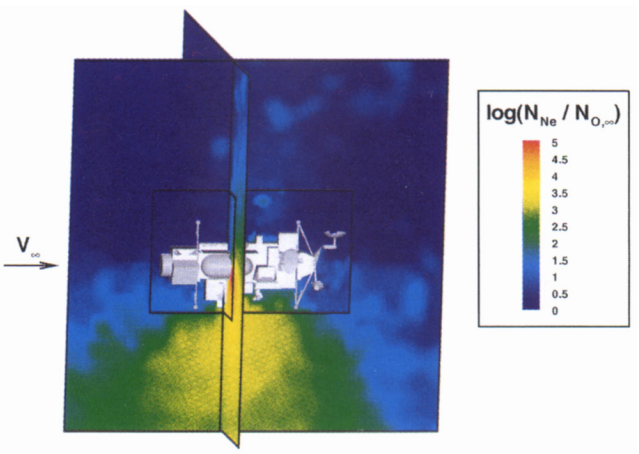

Fig. 4 Neon density map around UARS.

dependence of the outgassing flux rates was assumed to be given by the following equation[15]:

$$\phi(t) = \phi(t = 100°\text{C}) \exp\left(\frac{t - 100}{29}\right)$$

The collision cross section of each fictitious molecule is assumed to scale as the 2/3 power of its molecular mass, using monatomic oxygen as reference. The variable hard sphere (VHS) model[3] with a viscosity temperature coefficient of 0.75 is used to simulate collisions between molecules. Due to the lack of data, neither internal energy exchange nor chemistry is taken into account. The spacecraft surfaces are assumed to reflect molecules diffusely for both momentum and energy.

The CLAES vents are simulated as drifted Maxwellian free jets exhausting from sonic orifices at a temperature of 207 K. The other vents are assumed to be emitting gases with no bulk velocity.

The computational grid constructed around the satellite in the inner domain is shown in Fig. 1 for computational case 1. It is composed of 35,000 cells built on top of two background Cartesian meshes, with spatial resolutions of 15 and 5 cm. The outer computational domain for the grid is made of 7500 cells overlaid over a single Cartesian mesh of 30-cm resolution.

The spacecraft geometry is defined with 385 subelements, each one being a geometric primitive selected from the list shown in Table 1. Several instruments onboard UARS are free to rotate around pivot axes, such as the solar panel (one axis) and HALOE (two axes). Special coding has been introduced in the CAD preprocessor to allow for arbitrary angular positioning of these devices in order to study specific configurations of the space platform.

Characteristics of Contaminant Cloud Enveloping UARS

Figures 3–6 show the normalized number-density contour maps for atmospheric oxygen, neon, and $M = 100$ and $M = 200$ contaminant species for computational case 1. While contributions of each species are presented separately, all species coexist simultaneously in the simulation. Results are shown in two planes, the first one running longitudinally through the satellite, and the other perpendicular to the freestream. The black outline surrounding UARS denotes the boundary separating the inner and outer computational domains. Figure 3 shows that atmospheric oxygen accumulates on the windside of the vehicle with density reaching 50 times the freestream value.

The neon gas can be seen in Fig. 4 to expand like a plume, with surface reflection bending the jet outward. The $M = 100$ contaminant species can be seen to completely envelop the spacecraft, with

large concentrations extending in front of the satellite because of outgassing of adhesive material on the cell side of the solar panel. The $M = 200$ species is mostly emitted from the solar-panel shadow side and extends towards the rear of the spacecraft.

Contamination Level at HALOE Aperture

To ascertain the contaminant flux rates on HALOE optics and characterize the molecule stream incident on the telescope aperture, the simulation code uses a buffer file to store data on molecules entering HALOE, such as position and velocity vectors, species, and the number of previous collisions with the satellite surface and other molecules. From these molecular data, the velocity distribution function of each species incident on the HALOE aperture may be established, as shown in Fig. 7, which pertains to atmospheric atomic oxygen. The molecular velocity distribution of monatomic oxygen can be seen to be bimodal, with one mode centered at 7500 m/s, corresponding to unaffected freestream molecules, and the second mode representing molecules having suffered collisions with the satellite surface. The computed contamination flux deposition at the HALOE aperture may be seen in Table 4 for computational case 1. Results for computational cases 2 and 3 can be found in Refs. 13 and 14.

Assuming a 100% sticking coefficient, these fluxes correspond to a cumulative 35-month deposition thickness of 1500 and 1100 Å, respectively, for the $M = 100$ and $M = 200$ contaminant species. These deposition estimates are significantly lower than the ones obtained by Hatef,[15] who used the MOLFLUX analytical code and similar input conditions. The DSMC results corroborate on-orbit measurements revealing little optical degradation in the HALOE field of view.

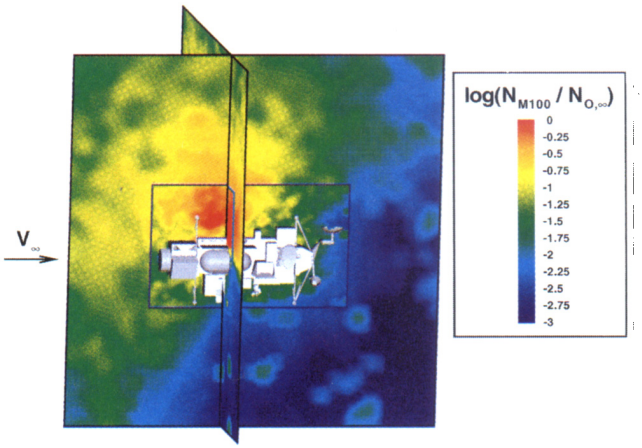

Fig. 5 Density map of $M = 100$ contaminant species.

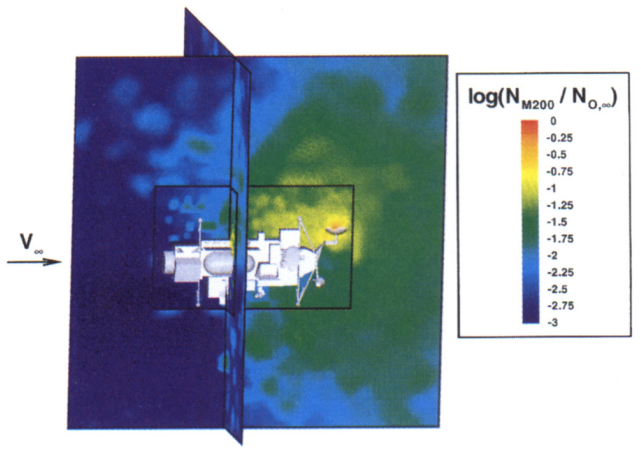

Fig. 6 Density map of $M = 200$ contaminant species.

Table 4 Mass flux rates incident at HALOE aperture[a]

Item	Mass flux rates, g/cm^2-s
Monatomic oxygen from freestream distribution	1.21×10^{-10}
Monatomic oxygen from surface-accommodated distribution	9.31×10^{-12}
Neon vented from CLAES experiment	1.86×10^{-11} (return flux) 1.33×10^{-11} (direct flux)
Carbon dioxide vented from CLAES experiment	$<5.79 \times 10^{-12}$[b]
Fictitious organic volatile species representing all GMW = 100 materials	9.20×10^{-14}
Fictitious organic volatile species representing GMW = 150 materials	3.94×10^{-15}
Fictitious organic volatile species representing GMW = 200 materials	4.26×10^{-13}

[a]Reference 14.
[b]No samples collected.

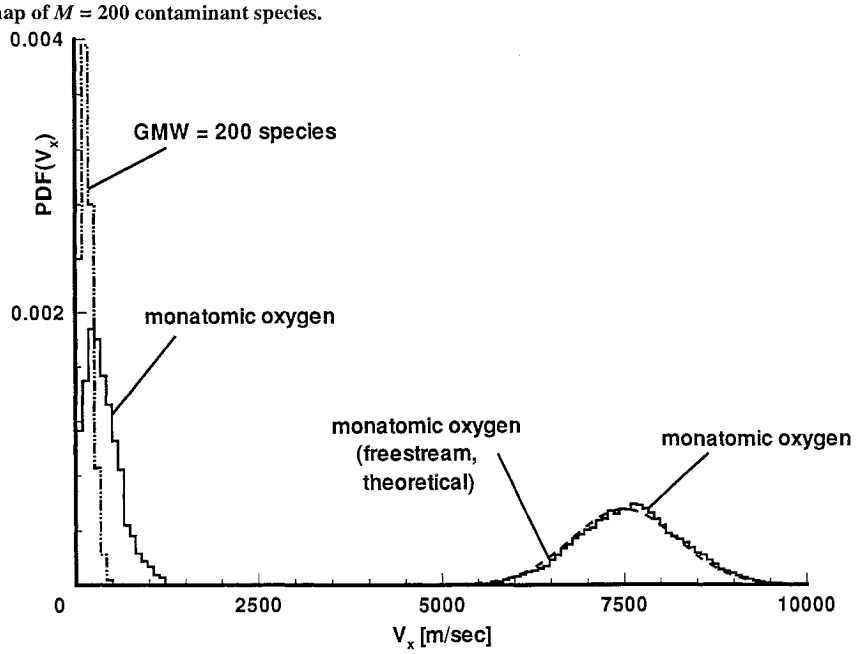

Fig. 7 Molecular velocity distribution at HALOE aperture.

Table 5 Simulation code performance

Computational domain	Inner	Outer
Number of simulated molecules	350,000	400,000
CPU runtime, h	190	150
RAM, Mbyte	60	40

Code Performance

The simulation has been performed on two Sun Sparc 2 workstations configured with 64 Mbyte of RAM and linked in a parallel virtual machine environment. Table 5 shows the code performance achieved for computational case 1. The long CPU runtimes are not necessary, but allow for improved statistics for the molecules incident on the HALOE aperture.

VII. Conclusion

The engineering community has long been relying on analytical codes to estimate the contamination level on spacecraft surfaces. These codes use geometric view factors to evaluate direct contamination fluxes, and rely on ad hoc models to allow for intermolecular collisions to estimate return fluxes. The DSMC approach is proposed here as an alternative tool. This approach has long been spurned by the contamination community because of its relative complexity, long run times, and inability to deal with the complex geometry of typical spacecraft and satellites. DSMC can, however, be very accurate in simulating collision dynamics and other pertinent physics, and is readily amenable to improvements through the introduction of new physical models (such as for surface deposition, momentum and energy accommodation, and gaseous-phase and surface chemistry) as more data become available through chamber tests and on-orbit measurements. Moreover, the DSMC algorithms and computer hardware (CPU speed and RAM) have now developed to the point where it is possible to perform DSMC simulation over bodies of extremely complex geometry on engineering desktop workstations with short turnaround times. This paper illustrates how the method can be applied to an actual spacecraft, namely the UARS satellite, to estimate contamination levels on a sensitive instrument, namely the HALOE telescope. DSMC will not supplant the much faster analytical codes, but should be used to either cross-check analytical-code results or perform high-accuracy contamination analysis for a set of spacecraft configurations that have been identified as mission-critical.

References

[1]Anon., "MOLFLUX—Molecular Flux User's Manual," NASA JSC-22496, Feb. 1989.

[2]Bird, G. A., *Molecular Gas Dynamics*, Clarendon, Oxford, England, UK, 1976.

[3]Bird, G. A., *Molecular Gas Dynamics and the Direct Simulation of Gas Flows*, Clarendon, Oxford, England, UK, 1994.

[4]Rault, D. F. G., "Aerodynamics of Shuttle Orbiter at High Altitudes," AIAA Paper 93-2815, July 1993.

[5]Bird, G. A., "Application of the Direct Simulation Monte Carlo Method to the Full Shuttle Geometry," AIAA Paper 90-1962, June 1990.

[6]Rault, D. F. G., Wilmoth, R. G., and Bird, G. A., "An Efficient DSMC Algorithm Applied to a Delta Wing," AIAA Paper 91-1316, June 1991.

[7]Rault, D. F. G., "Aerodynamic Characteristics of a Hypersonic Viscous Optimized Waverider at High Altitudes," AIAA Paper 92-0306, Jan. 1992.

[8]Rault, D. F. G., "Towards an Efficient Three-Dimensional DSMC Code for Complex Geometry Problems," 18th Rarefied Gas Dynamics Symposium, Vancouver, BC, Canada, July 1992.

[9]Rault, D. F. G., "Aerodynamic Characteristics of the Magellan Spacecraft in Venus Upper Atmosphere," AIAA Paper 93-0723, Jan. 1993.

[10]Moss, J. N., Rault, D. F. G., and Price, J. M., "DSMC Simulations of Hypersonic Viscous Interactions Including Separation," 18th Rarefied Gas Dynamics Symposium, Vancouver, BC, Canada, July 1992.

[11]Tartabini, P. V., Wilmoth, R. G., and Rault, D. F. G., "A Systems Approach to a DSMC Calculation of a Control Jet Interaction Experiment," AIAA Paper 93-2798, July 1993.

[12]Beguelin, A., Dongarra, J., Geist, A., Manchek, R., and Sunderam, V., "A User's Guide to PVM Parallel Virtual Machine," Oak Ridge National Lab., ORNL/TM-11826, July 1991.

[13]Woronowicz, M. S., and Rault, D. F. G., "On Predicting Contamination Levels of HALOE Optics Aboard UARS Using DSMC," AIAA Paper 93-2869, July 1993.

[14]Woronowicz, M. S., and Rault, D. F. G., "Direct Simulation Monte Carlo Prediction of On-Orbit Contamination Deposit for HALOE," NASA TM 109069, July 1994.

[15]Hatef, J. B., "Predicted Contamination of the HALOE," NASA TM-732-91-011.

I. D. Boyd
Associate Editor